Assessment of Steam Condensation Heat Transfer on Horizontal Tube Using MARS-KS and SPACE

Yeongjae Cho, Taeyeon Min, Jeong Ik Lee
Department of Nuclear and Quantum Engineering, Korea Advanced Institute of Science and Technology, 373-1 Guseong-dong Yuseong-gu, Daejeon 305-701, Republic of Korea
** Corresponding author: jeongiklee@kaist.ac.kr*

***Keywords: MARS-KS, SPACE, Heat Transfer, Condensation, Horizontal tube**

1. Introduction

Rapid expansion of artificial intelligence (AI)-driven digital infrastructure has significantly increased the demand for reliable and continuous electricity generation. Consequently, nuclear energy and Small Modular Reactors (SMRs) have been increased. SMRs have increasingly adopted integrated reactor configurations as helical tubes of steam generator to enhance heat transfer coefficient. The i-SMR also incorporates the helical-type steam generator inside the reactor vessel.

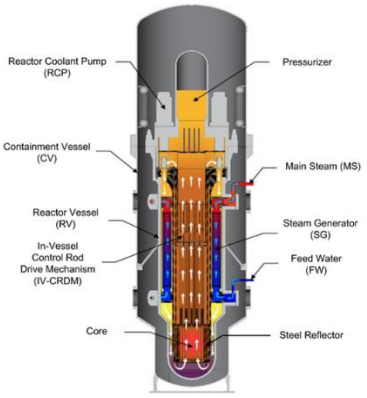

Fig. 1. Configuration of nuclear steam supply system and containment vessel referred from Lim [1]

Under accident conditions, steam condensation on the outer surface of steam-generator tubes could be presented and contributed to a critical role in residual heat removal. In certain i-SMR MMS charging pipe rupture accident scenarios, primary coolant discharged from the reactor coolant system evaporates, creating a steam environment around the steam-generator tubes. Therefore, accurately predicting external steam condensation on helical tubes in steam generators is essential for evaluating the heat-removal capability of passive safety systems.

The accuracy of the condensation heat-transfer models implemented in MARS-KS and SPACE can significantly influence the prediction of heat-removal performance. In particular, for condensation on a horizontal tube, the classical Nusselt film-condensation theory assumes gravity-dominated flow and neglects vapor-induced interfacial shear. However, as the vapor velocity increases, the condensate film can be affected by shear through the steam velocity effect and other flow-related effects, resulting in deviations from the gravity-dominated condensation behavior.

Therefore, as a preliminary step toward the analysis of external condensation on helically coiled tubes, the present study focuses on comparison of assessment of heat transfer for the steam condensation outside a horizontal tube using MARS-KS and SPACE. Moreover, the study further discusses the limitations of the condensation models implemented in each code and possible approaches for improving the accuracy of heat-transfer prediction under external condensation conditions.

2. Methodology

The horizontal-tube condensation configuration adopted in the present study was based on the experimental setup by Nobbs [2]. The MARS-KS and SPACE models were also designed the same geometry and thermal-hydraulic conditions from the Nobbs experiment. Accordingly, the heat-transfer parameters obtained from the experiment were compared with the corresponding values calculated by the two system codes to evaluate their predictive performance.

2.1. Experiment model

The experimental data and test model used in the present study were adopted from the experiment paper conducted by Nobbs [2].

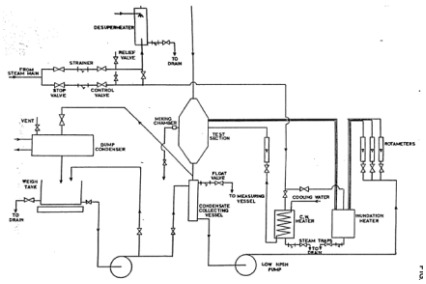

Fig. 2. Line Diagram of Experiment Facility referred from Nobbs [2]

Figure. 2 shows that the experiment rig from Nobbs.[2] For the condensation experiments on single horizontal tube, steam was introduced into a 0.5-m-long primary-side shell with a width of 95.25 mm under atmospheric-

pressure conditions, with vapor velocities ranging from 0.05 to 8.77 m/s. Cooling water was supplied through a 0.5-m-long tube with an outer diameter of 19.05 mm and an inner diameter of 15.875 mm. A total of 126 test cases were conducted, of which wall-temperature measurements were available for 42 cases.

2.2. MARS-KS and SPACE Modelling

Simplified modelling was chosen for the system-code analysis. Time-dependent volumes were used to specify the boundary conditions at the begging point of primary and second side. The primary side was modeled as a vertical shell pipe consisting of 10 nodes. A node sensitivity calculation was also performed for the horizontal tube in the test section using 10, 20, and 40 nodes. Since no significant differences were observed among the three nodalization schemes, the horizontal test section was modeled with 10 nodes to reduce computational cost. On the secondary side, the cooling water first passed through a 1-m-long entrance pipe to allow the flow to be developed before entering the horizontal tube of the test section. The corresponding MARS-KS and SPACE modeling configurations are shown in Figure. 3.

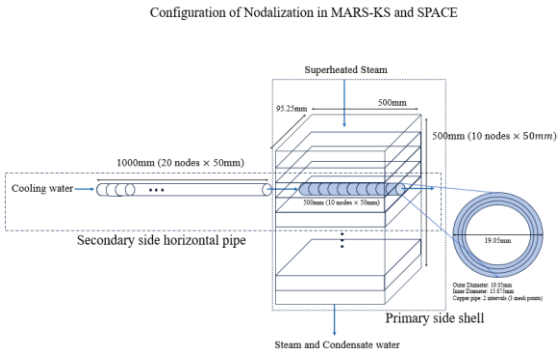

Fig. 3. Configuration of nodalization in MARS-KS and SPACE code for test section

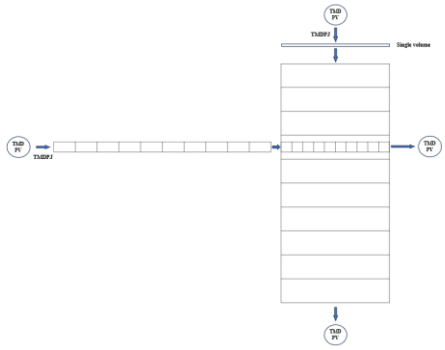

Fig. 4. Nodalization and Modelling in MARS-KS

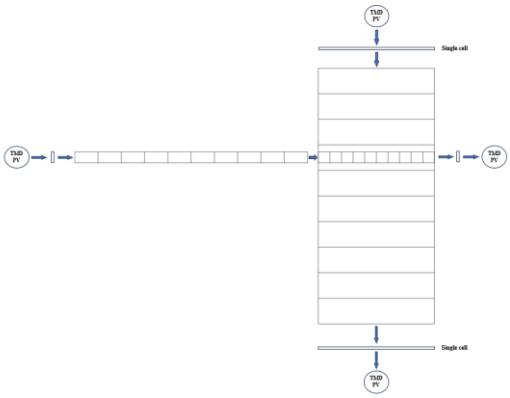

Fig. 5. Nodalization and Modelling in SPACE

Figure. 4 and 5 presents that the modeling and nodalization for MARS-KS and SPACE code.

Table. 1. The Ranges of Experimental Conditions and Input Parameters in MARS-KS and SPACE

Experimental condition/ Input parameter		Maximum	Minimum
1st Shell	Pressure (bar)	0.98	1.16
	Steam Inlet Temperature (K)	375	412
	Steam Inlet Velocity (m/s)	0.05	8.77
2nd pipe	Water Inlet Temperature (K)	284	340
	Water Flow rate (kg/s)	0.303	0.508

As shown in Table. 1, the experimental conditions represent the range of values covered by the 126 test cases, while the corresponding ranges of input parameters used in the MARS-KS and SPACE code simulations are also presented for comparison under the same conditions.

3. Steam Condensation Heat Transfer Model

The experimental and calculated results were compared using the dimensionless parameters proposed by Rose [3][4] and Nusselt.

The dimensionless F represents the relative importance of gravity-driven condensate drainage to the influence of vapor flow and is defined as

$$F = \frac{g D_o \mu_l h_{fg}}{U_\infty^2 k_l \left(T_{sat} - T_{wall,out}\right)} \quad (1)$$

where $g$is the gravitational acceleration, $D_o$is the outer tube diameter, $\mu_l$is the liquid viscosity, $h_{fg}$is the latent heat of vaporization, $U_\infty$is the free-stream vapor velocity, $k_l$is the condensation film thermal conductivity, T_{sat} is the saturation temperature, and $T_{wall,out}$is the outer wall temperature.

The parameter F represents the relative significance of gravity and vapor-flow effects on the condensate film. Large values of F correspond to gravity-dominated condensation, whereas decreasing F indicates an increasing contribution of vapor flow and interfacial shear from relatively high velocity of steam.

The condensation heat transfer coefficient for condensation film was expressed in terms of the Nusselt number,

$$Nu_{cond} = \frac{h_{cond} D_o}{k_l} \quad (2)$$

The Reynolds number for two-phases based on the Rose [3] was defined as

$$Re_{two-phase} = \frac{\rho_L U_\infty D_o}{\mu_{condensate}} \quad (3)$$

where ρ_L and μ_L are the condensate film density and vapor viscosity, respectively.

The normalized condensation heat transfer parameter was defined as by Rose [4]

$$Nu_{cond} Re_{two-phase}^{-0.5} = \frac{0.9 + 0.728F^{0.5}}{(1 + 3.44F^{0.5} + F)^{0.25}} \quad (4)$$

The Nusselt condensation model was defined as

$$Nu_{cond} Re_{two-phase}^{-0.5} = 0.728F^{0.25} \quad (5)$$

when $F \gg 1$, as the effect of vapor shear becomes insignificant because gravitational effects dominate the condensation process.

The convection heat transfer coefficient in the secondary pipe, which is used in Nobbs [2], based on Allen-Eckert equation was defined as

$$Nu_{cw} = 0.00127\, C_L Re_{cw} \mathrm{Pr}_{cw}^{0.42} (1 + 25\, Re_{cw}^{-0.27}) \left(\frac{\mu_{cw}}{\mu_{wall_{in}}}\right)^n \quad (6)$$

where C_L is a correction factor determined by the Prandtl number and the tube length-to-inner-diameter ratio (L/D_i), and n is an empirical exponent that depends on the flow development.

4. Results

4.1. Experimental F values and computed F values

To validate the applicability of the dimensionless parameter F which is calculated through the equations in Nobbs [2] to the entire dataset, the 42 cases for which the outer wall temperature was measured were firstly examined. For these cases, investigated F are directly obtained by using the equation (1) with the measured wall temperature is compared with computed F value obtained by using the heat-transfer coefficient calculation procedure in Nobbs [2] to calculate the outside wall temperature. The comparison is used to validate whether the calculated F values could be applied and set as a standard F value set for all 126 experiment cases.

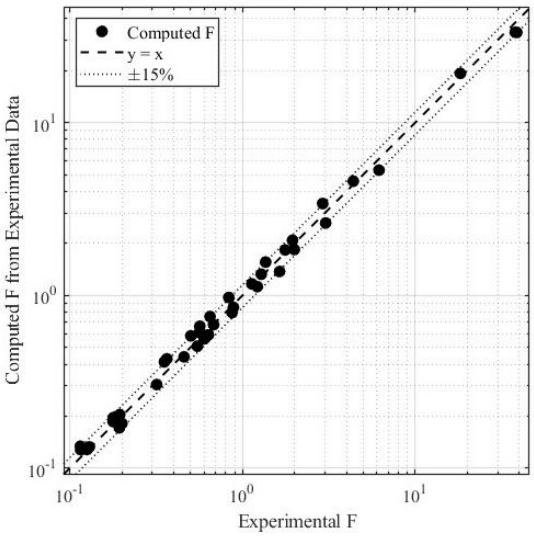

Fig. 6. Comparison of the experimental F values and computed F values

The average relative error between the experiment F value and calculated F value is 9.3%, while the maximum error is 17.6%, as shown in Fig. 6. Based on these results, the computed F values are considered applicable to the entire set of 126 experimental cases.

4.2. Exp vs. Code Predictions: Convective heat transfer coefficient

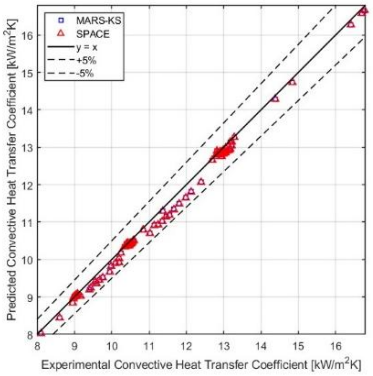

Fig. 7. Comparison of the convective heat transfer coefficients from experiment and code calculations

Figure. 7 compares the convective heat-transfer coefficients obtained from the Nobbs experiment [2], MARS-KS, and SPACE calculations. The coefficients are calculated by using the Allen–Eckert correlation in Eq. (6). It shows no significant differences among the experimental data and the two system-code prediction data through all results are presented within the ±5% error range. It indicates that convective heat transfer coefficient inside the secondary-side is predicted consistently by MARS-KS and SPACE.

4.3. Exp vs. Code Predictions: Condensation heat transfer coefficient

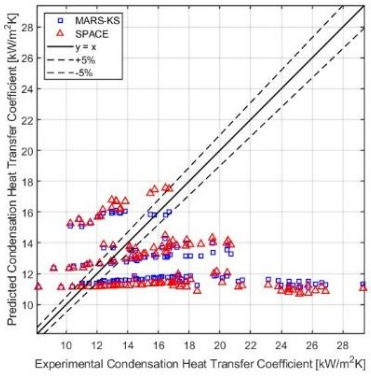

Fig. 8. Comparison of the condensation heat transfer coefficients from experiment and code calculations

Figure. 8 compares the condensation heat transfer coefficients predicted by MARS-KS and SPACE with experimental condensation heat transfer coefficients. Those codes predict condensation heat transfer coefficients primarily in the range of 10 to 18 kW/m²·K, whereas the experimental values are distributed over a substantially wider range of approximately between 10 and 30 kW/m²·K. This indicated that the condensation heat transfer coefficient was predicted with relatively low accuracy.

4.4. Comparison of Condensation Heat Transfer Coefficient with Respect to F

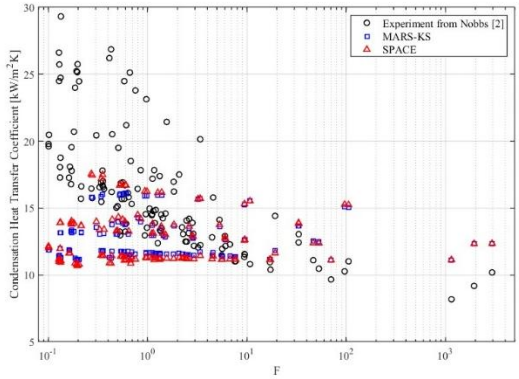

Fig. 9. Comparison of condensation heat transfer coefficient with respect to $\boldsymbol{F}$

Figure. 9 presents the condensation heat transfer coefficients from code calculation and experiment with respect to F values. Both MARS-KS and SPACE considerably underestimate the condensation heat transfer coefficient in the low F number region, particularly for its range up to approximately 10. This discrepancy indicates that the two codes do not sufficiently consider vapor shear effect. In contrast, at relatively high values of F number above approximately 20, the predicted condensation heat transfer coefficients from both MARS-KS and SPACE tend to exceed the experimental values. This overestimation is considered to result from the one-dimensional system codes selecting the higher condensation heat transfer coefficient predicted by the Nusselt model which is used in analysis codes.

4.4. Comparison of the Normalized Condensation Heat Transfer Parameter with Respect to F

The condensation heat transfer coefficient could be expressed from Eq. (2). Moreover, the normalized condensation heat transfer parameter is defined by using two-phases Reynolds number in Eq. (3). The dimensionless heat transfer parameter, $Nu/Re_v^{1/2}$, enables the condensation heat transfer behavior under different vapor-flow conditions to be compared using a unified dimensionless relationship. Therefore, this paper conducts the comparison of $Nu/Re_v^{1/2}$ against F.

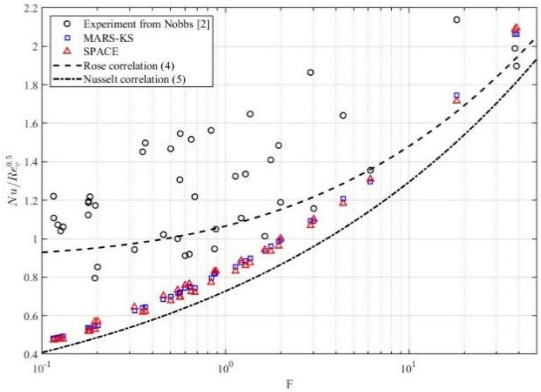

Fig. 10. Comparison of $\boldsymbol{Nu/Re_v^{1/2}}$ with respect to the experimental $\boldsymbol{F}$ values (42 cases)

Figure. 10 presents comparison of dimensionless condensation heat transfer parameter with respect to the experimental F values among 42 cases. Two code underpredicts the $Nu/Re_v^{1/2}$ values in low F value regions. Moreover, in the low F region, the normalized condensation heat transfer coefficients were closer to the Nusselt correlation than to the Rose correlation.

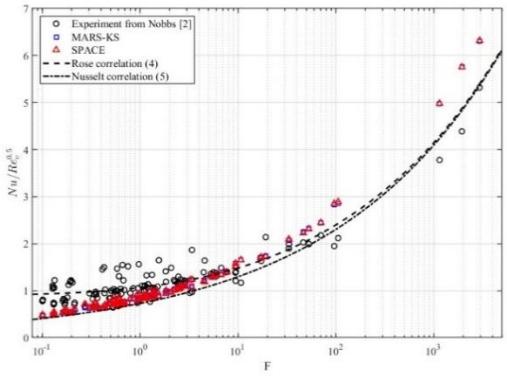

Fig. 11. Comparison of $\boldsymbol{Nu/Re_v^{1/2}}$ with respect to the computed $\boldsymbol{F}$ values (126 cases)

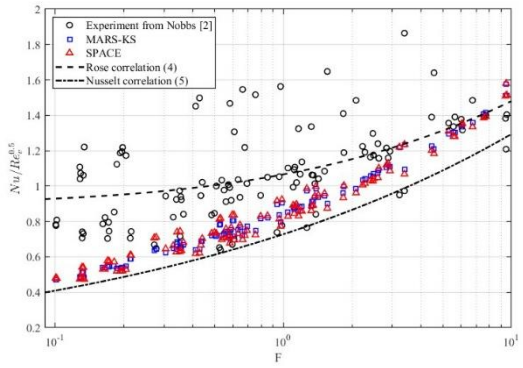

Fig. 12. Comparison of $Nu/Re_v^{1/2}$ with respect to the computed F values from 10^{-1} *to* 10

Figure. 11 and Figure. 12 compare the dimensionless heat transfer parameter obtained from the experimental data and calculated data by MARS-KS, SPACE with respect to the computed F values. As the experimental F value increases, the dimensionless condensation heat transfer parameter exhibits an increasing trend, which is successfully preseneted by both MARS-KS and SPACE.

In the low F value region, however, both codes underpredict the dimensionless condensation heat transfer parameter as shown in Fig. 11 and Fig. 12. Moreover, As discussed previously about Figure. 10, which focuses on the low F region, shows that the normalized condensation heat transfer coefficient were closer to the Nusselt correlation than to the Rose correlation. This underprediction is considered to result from the limited ability of the condensation models to account for vapor shear effects.

At intermediate F values around 10, these codes shows relatively predict close to the experimental data. In contrast, for high F values above approximately 20, these codes tend to overestimate the dimensionless condensation heat transfer parameter. This overprediction is considered to be associated with the model selection approach implemented in the codes.

4. Summary and Conclusions

This study is conducted as a preliminary investigation to improve the validation of condensation heat transfer in MARS-KS and SPACE for analyzing condensation on helically coiled steam generator tubes under i-SMR accident conditions. The experimental model developed by Nobbs [2] was selected as the reference case for validating the condensation heat transfer models implemented in MARS-KS and SPACE.

The convective heat transfer coefficients predicted by two selected codes show no significant differences from the experimental values. In contrast, noticeable discrepancies are observed in the condensation heat transfer coefficients, with these codes tending to underpredict at low F region and overpredict at high F region. Also, for the normalized condensation heat transfer parameter, both codes underpredict at low F region and overpredict at high F region. These results suggest that the Nusselt condensation models currently used in the analysis codes may not sufficiently account for conditions where vapor-induced interfacial shear is significant. Therefore, applying condensation models that explicitly consider vapor shear effects is expected to improve prediction accuracy.

The present results can serve as a basis for improving condensation heat transfer models for application to helically coiled steam generator tubes under i-SMR accident conditions.

ACKNOWLEDGE

This work was supported by the Innovative Small Modular Reactor Development Agency grant funded by the Korea Government (MCEE) (No. RS-202400404240).

REFERENCES

[1] Lim, S. G., Nam, H. S., Lee, D. H., & Lee, S. W. (2025). Design characteristics of nuclear steam supply system and passive safety system for Innovative Small Modular Reactor (i-SMR). *Nuclear Engineering and Technology*, *57*(10), 103697.
[2] Nobbs, D. W. (1975). The Effect of Downward Vapour Velocity and Inundation on the Condensation Rates on Horizontal Tubes and Tube Tanks.
[3] Lee, W. C., & Rose, J. W. (1984). Forced convection film condensation on a horizontal tube with and without non-condensing gases. *International journal of heat and mass transfer*, *27*(4), 519-528.
[4] Rose, J. W. (1984). Effect of pressure gradient in forced convection film condensation on a horizontal tube. *International journal of heat and mass transfer*, *27*(1), 39-47.